# Inter-layer Potential for Hexagonal Boron Nitride

# Supplementary Material

*Itai Leven,[1] Ido Azuri,[2] Leeor Kronik,[2] and Oded Hod[1,\*]*

[1] Department of Chemical Physics, School of Chemistry, the Raymond and Beverly Sackler Faculty of Exact Sciences, Tel-Aviv University, Tel-Aviv 69978, Israel

[2] Department of Materials and Interfaces, Weizmann Institute of Science, Rehovoth 76100, Israel

## A.  Charges

In order to evaluate the performance of the electronegativity equalization method (EEM)[1-5] for *h*-BN we compare the effective atomic charges obtained using the EEM with our parameterization for a set of B-N-H molecules to Mulliken atomic charges obtained at the B3LYP/6-31G** level of theory as implemented in the Gaussian suite of programs.[6,7] In what follows, all charges are given in units of the elementary charge. As can be seen below, good agreement between the first principles results and the EEM is obtained for all molecules considered using our parameterization.
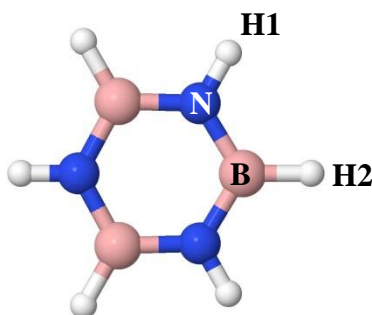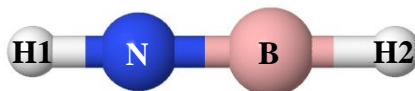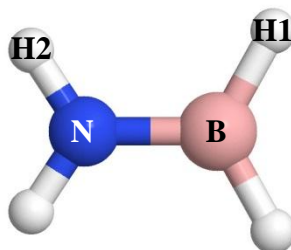
**Borazine:**



Figure S1: Definition of various atomic positions in the borazine molecule

| Atom | B3LYP | EEM |
|:---:|:---:|:---:|
| **B** | 0.30 | 0.32 |
| **N** | -0.47 | -0.5 |
| **H1** | 0.25 | 0.19 |
| **H2** | -0.08 | -0.01 |

Table S1: Partial effective atomic chargers of borazine as calculated via DFT at the B3LYP/6-31G** level of theory using the Mulliken charge analysis and the re-parameterized EEM method.

**BNH$_2$:**



Figure S2: Definition of various atomic positions in the BNH$_2$ molecule

| Atom | B3LYP | EEM |
|:---:|:---:|:---:|
| **B** | 0.14 | 0.22 |
| **N** | -0.4 | -0.47 |
| **H1** | 0.26 | 0.26 |
| **H2** | 0.0 | 0.01 |

Table S2: Partial effective atomic chargers of BNH$_2$ as calculated via DFT at the B3LYP/6-31G** level of theory using the Mulliken charge analysis and the re-parameterized EEM method.
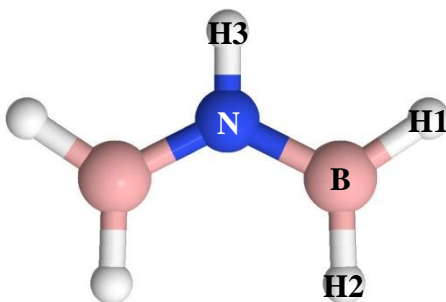
**BNH$_4$:**



Figure S3: Definition of various atomic positions in the BNH$_4$ molecule

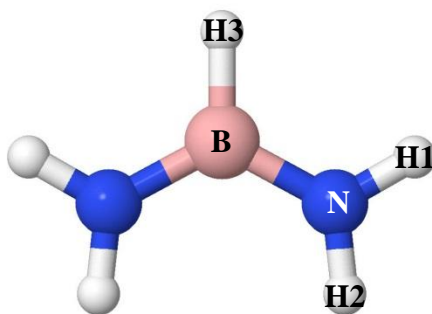| Atom | B3LYP | EEM |
|:---:|:---:|:---:|
| **B** | 0.16 | 0.18 |
| **N** | -0.53 | -0.57 |
| **H1** | -0.07 | -0.01 |
| **H2** | 0.26 | 0.2 |

Table S3: Partial effective atomic chargers of BNH$_4$ as calculated via DFT at the B3LYP/6-31G** level of theory using the Mulliken charge analysis and the re-parameterized EEM method.

**H₂B-NH-BH₂:**



Figure S4: Definition of various atomic positions in the $B_2NH_5$ molecule

| Atom | B3LYP | EEM |
|:---:|:---:|:---:|
| B | 0.19 | 0.18 |
| N | -0.39 | -0.52 |
| H1 | -0.07 | -0.01 |
| H2 | -0.05 | 0.0 |
| H3 | 0.25 | 0.21 |

Table S4: Partial effective atomic chargers of $B_2NH_5$ as calculated via DFT at the B3LYP/6-31G** level of theory using the Mulliken charge analysis and the re-parameterized EEM method.

**H₂N-BH-NH₂:**



Figure S5: Definition of various atomic positions in the $N_2BH_5$ molecule

| Atom | B3LYP | EEM |
|:---:|:---:|:---:|
| N | -0.6 | -0.56 |
| B | 0.35 | 0.31 |
| H1 | 0.23 | 0.21 |
| H2 | 0.25 | 0.19 |
| H3 | -0.1 | 0.0 |

Table S5: Partial effective atomic chargers of $BN_2H_5$ as calculated via DFT at the B3LYP/6-31G** level of theory using the Mulliken charge analysis and the re-parameterized EEM method.

# B.   B-N-H ReaxFF parameters:

In the present implementation, the *h*-BN ILP is used in conjunction with the ReaxFF for describing the intra-layer interactions of molecular *h*-BN derivatives. According to our calculations, the original ReaxFF parameterization, as presented in Ref. 8, somewhat overestimates the optimal B-N bond length in the borazine molecule giving a value of 1.5 Å as compared to the B3LYP/6-31G** value of 1.43 Å. Furthermore, this set of parameters results in qualitatively and quantitatively poor torsional strain energy curves for the $BNH_4$ molecule compared to those obtained from DFT calculations. Therefore, in order to improve the description of the ReaxFF for the intra-layer interactions in *h*-BN molecular derivatives, the parameterization of the ReaxFF for B-N-H molecular systems presented in Ref. 8 is somewhat modified. We note that this re-parameterization is performed with the aim to maintain the good agreement between ReaxFF and first-principles results as obtained in the original derivation of the force field. In what follows, we present the modified parameters corresponding to the ReaxFF equations as described in Ref. 9. The original value of each modified parameter is given in red in parentheses for comparison purposes. In the next section, the performance of the force filed with the modified parameters is demonstrated.

## General parameters:

| Atom | Mass (a.m.u) | Val | $Val_e$ | $Val_{boc}$ | $n_{lp,opt}$ |
|:---:|:---:|:---:|:---:|:---:|:---:|
| **H** | 1.0080 | 1.0 | 1.0 | 1.0 | 0.0 |
| **B** | 10.811 | 3.0 | 3.0 | 3.0 | 0.0 |
| **N** | 14.0 | 3.0 | 5.0 | 4.0 | 1.0 |

Table S6: General parameter values used in the ReaxFF force field for B-N-H molecules.

| | | | |
|:---:|:---:|:---:|:---:|
| $\lambda_1(P_{boc1})$ | 50.0 | $\lambda_{21}(P_{pen3})$ | 0.3989 |
| $\lambda_2(P_{boc2})$ | 9.4569 | $\lambda_{22}(P_{pen4})$ | 3.9954 |
| $\lambda_3(P_{coa2})$ | 56.6636 | $\lambda_{23}$ | - |

| | | | |
|---|---|---|---|
| $\lambda_4(P_{trip4})$ | 3.0 | $\lambda_{24}(P_{ptor2})$ | 5.8374 |
| $\lambda_5(P_{trip3})$ | 6.5 | $\lambda_{25}(P_{ptor3})$ | 10.0 |
| $\lambda_6(kc2)$ | 50.0 | $\lambda_{26}(P_{ptor4})$ | 1.882 |
| $\lambda_7(P_{ov/un6})$ | 1.0701 | $\lambda_{27}$ | - |
| $\lambda_8(P_{trip2})$ | 15.0 | $\lambda_{28}(P_{cot2})$ | 2.1861 |
| $\lambda_9(P_{ov/un7})$ | 11.9083 | $\lambda_{29}(P_{vdW1})$ | 1.5591 |
| $\lambda_{10}(P_{ov/un8})$ | 13.3822 | $\lambda_{30}(BO_{cuttoff})$ | 0.01 |
| $\lambda_{11}(P_{trip1})$ | -24.671 | $\lambda_{31}(P_{coa4})$ | 0.7151 |
| $\lambda_{12}(swa)$ | 0.0 | $\lambda_{32}(P_{ov/un4})$ | 2.7425 |
| $\lambda_{13}(swb)$ | 20.0 (10.0) | $\lambda_{33}(P_{ov/un3})$ | 12.5819 |
| $\lambda_{14}$ | - | $\lambda_{34}(P_{val8})$ | 2.1533 |
| $\lambda_{15}(P_{val6})$ | 33.8667 | $\lambda_{35}$ | - |
| $\lambda_{16}(P_{lp1})$ | 5.8971 | $\lambda_{36}$ | - |
| $\lambda_{17}(P_{val9})$ | 1.0563 | $\lambda_{37}$ | - |
| $\lambda_{18}(P_{val10})$ | 2.0384 | $\lambda_{38}$ | - |
| $\lambda_{19}$ | - | $\lambda_{39}(P_{coa3})$ | 1.4155 |
| $\lambda_{20}(P_{pen2})$ | 6.929 | | |

Table S7: General parameter values used in the ReaxFF force field for B-N-H molecules.

## Bond order term:

| Bond | $P_{bo1}$ | $P_{bo2}$ | $P_{bo3}$ | $P_{bo4}$ | $P_{bo5}$ | $P_{bo6}$ |
|---|---|---|---|---|---|---|
| **HH** | -0.0113 | 5.6991 | - | - | - | - |
| **BB** | -0.0691 | 5.8065 (5.0065) | -0.2 | 15.0 | - | - |
| **BH** | -0.0722 | 6.255 (5.1245) | - | - | - | - |
| **BN** | -0.165 | 7.0248 (6.5248) | -0.2935 | 10.2737 | - | - |
| **NN** | -0.1884 | 7.7 (5.6414) | -0.4426 | 8.2367 | -0.282 | 12.0357 |
| **NH** | -0.0491 | 6.4 (5.7202) | - | - | - | - |

Table S8: Parameter values used in the bond order term of the ReaxFF force field for B-N-H molecules.

| Bond | $r_0^\sigma$(Å) | $r_0^\pi$(Å) | $r_0^{\pi\pi}$(Å) | $D_e^\sigma$(Kcal / mol) | $D_e^\pi$(Kcal / mol) | $D_e^{\pi\pi}$(Kcal / mol) |
|------|------|------|------|------|------|------|
| HH | 0.6867 | - | - | 165.7021 | - | - |
| BB | 1.3484 | 1.0 | - | 109.1015 | - | - |
| BH | 1.1948 (1.1648) | - | - | 167.4103 (177.4103) | - | - |
| BN | 1.38 (1.4037) | 1.2273 (1.2073) | - | 153.9715 (143.9715) | 94.2037 | - |
| NN | 1.39 (1.552) | 1.2641 | 1.12 (1.0972) | 135.587 (104.5870) | 85.8215 | 151.8152 |
| NH | 1.065 (0.9496) | - | - | 231.8918 | - | - |

Table S9: Parameter values used in the bond order term of the ReaxFF force field for B-N-H molecules.

| Bond | F1(ovc) | $P_{be1}$ | $P_{be2}$ | Atom | $P_{boc3}$ | $P_{boc4}$ | $P_{boc5}$ |
|------|------|------|------|------|------|------|------|
| HH | 0 | -0.8328 | 6.5603 | H | 3.2094 (4.8714) | 3.9714 (6.1752) | 0.0009 |
| BB | 1 | 1.0 | 0.8313 | B | 4.5 (6.8208) | 3.6 (4.0943) | 1.0943 |
| BH | 1 | -0.4601 | 9.2806 | N | 2.0645 (2.7645) | 2.5862 | 2.6432 |
| BN | 1 | 0.2868 | 0.5585 | | | | |
| NN | 1 | -0.9395 | 0.3279 | | | | |
| NH | 0 | -0.7398 | 9.1469 | | | | |

Table S10: Parameter values used in the bond order term of the ReaxFF force field for B-N-H molecules.

## Lone pair term:

| Atom | $P_{lp2}$ |
|------|------|
| H | 0.0 |
| B | 0.0 |
| N | 29.92 |

Table S11: Parameter values used in the lone-pair term of the ReaxFF force field for B-N-H molecules.

## Over/Under-coordination term:

| Bond | $P_{ov/un1} \left(\frac{Kcal}{mol}\right)$ | Atom | $P_{ov/un2}$ | $P_{ov/un5}$ |
|------|------|------|------|------|
| HH | 0.3597 | H | -15.7683 | 0.0 |
| BB | 0.1 | B | -3.6082 | 7.2404 |
| BH | 0.4971 | N | -6.434 | 27.4217 |
| BN | 0.1083 | | | |
| NN | 1.0 | | | |
| NH | 0.4224 | | | |

Table S12: Parameter values used in the over/under coordination term of the ReaxFF force field for B-N-H molecules.

## Valance Angle term:

| Angle | $P_{val1}$ | $P_{val2}$ | $P_{val4}$ | $P_{val7}$ | $\theta_{0,0}$ ° | Atom | $P_{val3}$ |
|-------|-----------|-----------|-----------|-----------|----------|------|-----------|
| NNH | 28.255 (24.255) | 2.3034 | 1.04 | 0.1 | 82.7 (72.7618) | H | 2.1504 |
| HNH | 30.9831 (27.9831) | 4.0538 | 1.2487 | 0.7544 | 79.5836 (85.5836) | B | 1.8 |
| NNN | 20.6158 | 3.9104 | 1.05 | 1.7772 | 73.9146 | N | 2.6491 |
| HNB | 30.9131 (14.9131) | 0.529 | 1.04 | 0.1 | 60.0 (55.0) | Atom | $P_{val5}$ |
| BNB | 30.87 | 0.844 | 1.0576 | 3.0 | 47.0 (50.0) | H | 2.8793 |
| NNB | 40.0 | 4.0 | 1.25 | 1.0 | 70.0 | B | 2.8413 |
| NHH | 10.0019 | 1.0 | 1.04 | 0.0 | 0.0 | N | 2.8793 |
| NHN | 5.0 | 2.0 | 1.04 | 0.0 | 0.0 | | |
| HHH | 27.9213 | 5.8635 | 1.04 | 0.0 | 0.0 | | |
| BHB | 5.0 | 1.0 | 1.04 | 1.0 | 0.0 | | |
| BHH | 5.0019 | 1.0 | 1.5 | 0.0 | 0.0 | | |
| NHB | 9.698 | 1.0 | 1.04 | 1.0 | 0.0 | | |
| HBB | 32.2012 | 4.7029 | 1.04 | 3.0 | 59.0 (55.0) | | |
| BBB | 35.0 | 3.0 | 1.01 | 1.5 | 70.0 | | |

| | | | | | |
|---|---|---|---|---|---|
| **NBN** | 40.0571 (38.0571) | 4.2562 | 1.3861 | 1.1083 | 65.3075 (72.3075) |
| **NBB** | 40.0 | 6.0 | 1.04 | 3.0 | 50.0 |
| **HBN** | 2.5 | 0.1 | 2.2627 | 0.1 | 48.0 (55.0) |
| **HBH** | 14.6089 | 2.3811 | 3.0 | 3.0 | 57.5987 (62.5987) |

Table S13: Parameter values used in the valence angle term of the ReaxFF force field for B-N-H molecules.

## Torsion angle:

| Atom | $V1\left(\frac{Kcal}{mol}\right)$ | $V2\left(\frac{Kcal}{mol}\right)$ | $V3\left(\frac{Kcal}{mol}\right)$ | $P_{tor1}$ | $P_{cot1}$ |
|---|---|---|---|---|---|
| **XBBX** | 0.25 | 50.0 | 0.3 | -7.5 | 0.0 |
| **XBNX** | -2.0 | 90.3351 (19.3351) | 0.3228 | -3.4735 (-5.4735) | 0.0 |
| **XBHX** | 0.0 | 0.0 | 0.0 | 0.0 | 0.0 |
| **XHHX** | 0.0 | 0.0 | 0.0 | 0.0 | 0.0 |
| **XHNX** | 0.0 | 0.1 | 0.02 | -2.5415 | 0.0 |
| **XNNX** | -2.0 | 88.4048 (24.4048) | -0.2617 | -3.3327 | -2.0 |

Table S14: Parameter values used in the torsion angle term of the ReaxFF force field for B-N-H molecules.

## Intra-layer van der-Waals term:

In addition to the vdW energy term detailed in Ref. 9 ($E_{vdW}$), the LAMMPS code implementation adds an inner shield function.[12,13] The functional form of this shield function is:

$$Inner\ shield = e_{core} + e^{\left(a_{core}\cdot\left(1-\frac{r_{ij}}{r_{core}}\right)\right)}$$

and the final form of the intra-layer vdW term is given by:

$$E_{vdw}^{LAMMPS} = Tap \cdot (E_{vdW} + inner\ shield)$$

In the following table, we present the parameters of $E_{vdW}$ and the inner shield term that are used in our implementation.

| Atom | $\alpha$ | $r_{vdW}$(Å) | $D_{vdW}\left(\frac{Kcal}{mol}\right)$ | Atom | $r_{core}$ | $e_{core}$ | $a_{core}$ | $\gamma_W$(Å) |
|------|----------|--------------|------------------------------------------|------|------------|------------|------------|----------------|
| HH | 9.385 | 1.3525 | 0.0616 | H | 0.6 | 0.1 | 10.0 | 5.0013 |
| BB | 12.4662 | 1.65 (1.8276) | 0.05 | B | 1.4 | 0.1 | 12.0 | 2.6721 |
| BH | 11.2019 | 1.501 | 0.0566 (0.526) | N | 1.4 | 0.1 | 10.0 | 7.6886 |
| BN | 10.7561 | 1.7 | 0.0564 | | | | | |
| NN | 10.0667 | 1.7695 | 0.1375 | | | | | |
| NH | 10.5106 | 1.647 | 0.0567 (0.0367) | | | | | |

Table S15: Parameter values used in the intra-layer van der-Waals term of the ReaxFF force field for B-N-H molecules.

## Coulomb term:

| Atom | $\chi(eV)$ | $\eta(eV)$ | $\gamma$(Å) |
|------|------------|------------|-------------|
| H | 10.2 (6.5362) | 7.0327 | 0.8 (0.7492) |
| B | 13.0 (6.8775) | 6.7020 | 0.7 (0.9088) |
| N | 10.0 (8.1308) | 7.0 | 0.69 (1.0) |

Table S16: Parameter values used in the Coulomb term of the ReaxFF force field for B-N-H molecules.

# C.  Intra-layer B-N-H Molecular Benchmark Tests

Here, we present benchmark tests for the performance of the ReaxFF using the new set of parameters as detailed above for describing various equilibrium geometries, bond dissociation energies, valance angles strain, and torsional angles strain of several B-N-H molecules. The DFT data presented below is taken from Refs. 8,10,11 and our own calculations utilizing the Gaussian suit of programs[7,12] at the B3LYP/6-31G** level of theory. The Benchmark tests are carried out by an initial optimization of the molecular structure followed by single point calculations at each strained configuration. In what follows, we present results of our calculations using our local implementation of the ReaxFF with the modified parameters against results of the original ReaxFF implementation within the LAMMPS code [13,14] and the DFT results.

## Molecular geometries:

We start by comparing optimal bond lengths and valence angles of various B-N-H molecules, including borazine, which can be thought of as the smallest *h*-BN molecular derivative, as obtained using DFT, the LAMMPS code,[13,14] and our implementation of the ReaxFF with the modified parameters presented above. As can be seen in Tab. 17 below, in most cases considered our new parameterization results in improved agreement with the first-principle geometries as compared to the LAMMPS results.

| Molecule | Angle/Bond | DFT* | Our parameterization | LAAMPS |
|---|---|---|---|---|
| **H2B-BH2** | | | | |
| | B-B(A) | 1.74 | 1.76 | 1.89 |
| | B-H(A) | 1.19 | 1.16 | 1.16 |
| | < H-B-H(degrees) | 116.20 | 117.27 | 110.35 |
| **BH3** | | | | |
| | B-H(A) | 1.19 | 1.17 | 1.17 |
| | < H-B-H(degrees) | 120.00 | 120.00 | 120.00 |
| **B3N3H6 (borazine)** | | | | |
| | B-N(A) | 1.43 | 1.45 | 1.50 |
| | B-H(A) | 1.19 | 1.19 | 1.18 |
| | N-H(A) | 1.01 | 1.00 | 0.89 |

| | | | | |
|---|---|---|---|---|
| | < B-N-B(degrees) | 122.90 | 122.50 | 122.40 |
| | < N-B-N(degrees) | 117.10 | 117.45 | 117.50 |
| **H2B-NH2** | | | | |
| | B-N(A) | 1.39 | 1.43 | 1.40 |
| | B-H(A) | 1.19 | 1.18 | 1.18 |
| | N-H(A) | 1.01 | 1.02 | 0.96 |
| | < H-B-H(degrees) | 119.90 | 118.40 | 118.60 |
| | < H-B-N(degrees) | 121.80 | 120.70 | 120.60 |
| | < H-N-B(degrees) | 123.20 | 126.60 | 116.50 |
| | < H-N-H(degrees) | 113.40 | 106.70 | 109.60 |
| **HB-NH** | | | | |
| | B-N(A) | 1.23 | 1.20 | 1.22 |
| | B-H(A) | 1.17 | 1.17 | 1.18 |
| | N-H(A) | 0.99 | 0.98 | 0.90 |
| | < H-B-N(degrees) | 180.00 | 180.00 | 174.40 |
| **H2B-NH-BH2** | | | | |
| | B-N(A) | 1.42 | 1.44 | 1.43 |
| | B-H(A) | 1.19 | 1.18 | 1.18 |
| | N-H(A) | 1.02 | 1.00 | 0.90 |
| | < B-N-B(degrees) | 126.40 | 128.70 | 125.50 |
| **H2N-BH-NH2** | | | | |
| | B-N(A) | 1.42 | 1.42 | 1.43 |
| | B-H(A) | 1.20 | 1.19 | 1.19 |
| | N-H(A) | 1.01 | 1.02 | 0.96 |
| | < N-B-N(degrees) | 123.20 | 120.20 | 120.20 |
| **Molecule** | **Angle/Bond** | **DFT\*\*** | **Our code** | **LAMMPS** |
| **H2N-NH2** | | | | |
| | N-N(A) | 1.49 | 1.48 | 1.51 |
| | N-H(A) | 1.02 | 1.01 | 0.98 |
| | < N-N-H(degrees) | 103.30 | 104.50 | 110.70 |
| | < H-N-H(degrees) | 102.20 | 107.20 | 111.30 |
| **NN** | | | | |
| | N-N(A) | 1.11 | 1.10 | 1.09 |
| **HNNH** | | | | |
| | N-N(A) | 1.25 | 1.25 | 1.24 |
| | N-H(A) | 1.04 | 1.01 | 0.90 |
| | < H-N-N(degrees) | 106.00 | 112.00 | 119.60 |

\* DFT data from reference 10.

\*\* DFT data from reference 11.

Table S17: Equilibrium geometrical parameters obtained using the ReaxFF with the original parameterization, the modified parameters, and DFT benchmark calculations.

# B-B bond dissociation in $B_2H_4$:

The dissociation curve of the B-B bond in the $B_2H_2$ molecule as calculated using the modified ReaxFF parameters (left panel of Fig. S6) fits well the original parameterization results, as well as DFT benchmark data, calculated at the B3LYP/6-311G** level of theory, of Ref. 10 (right panel of Fig. S6).
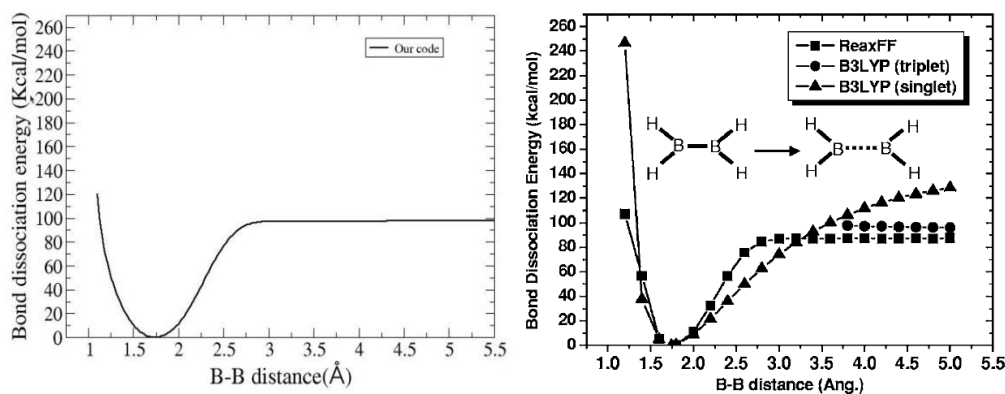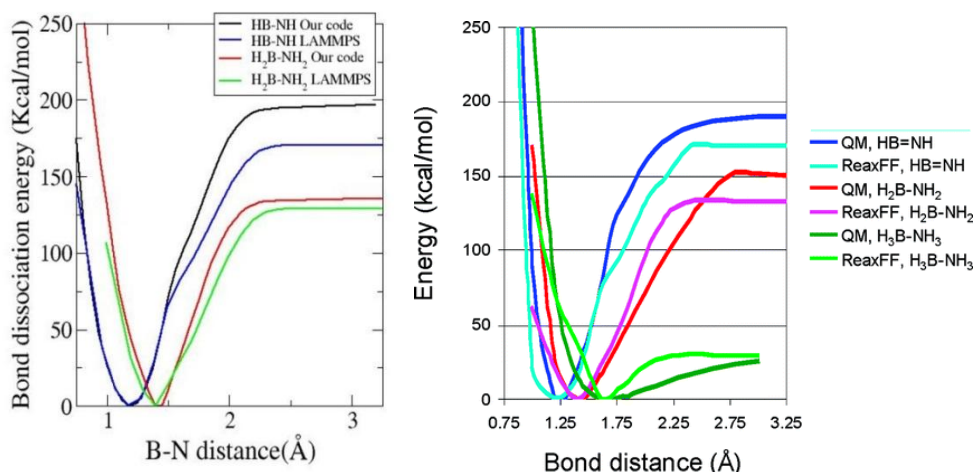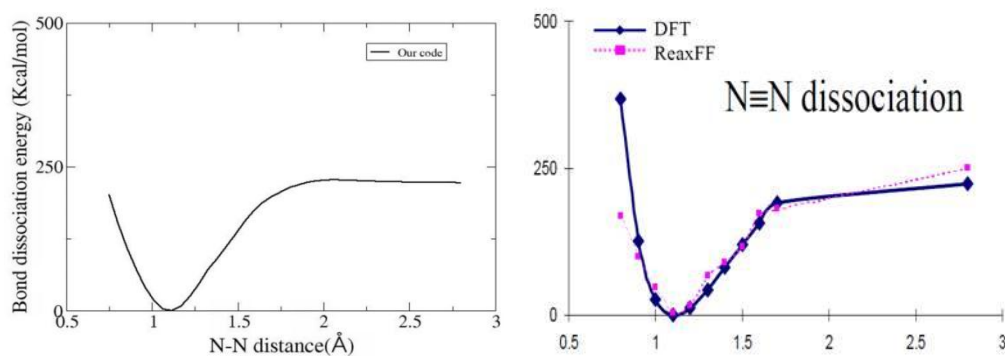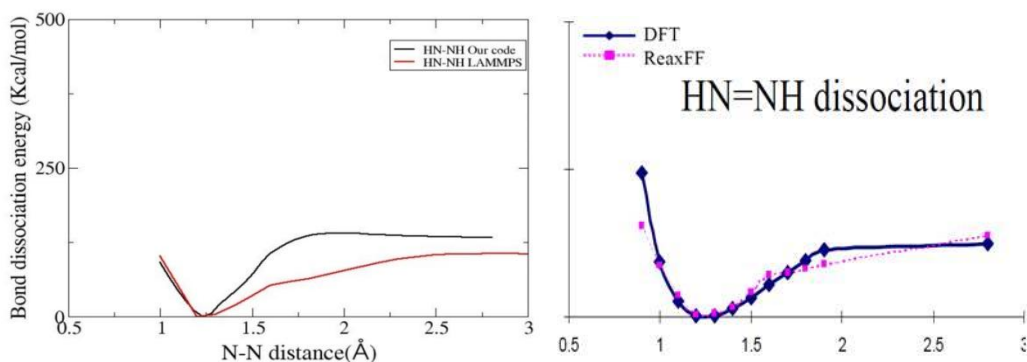


Figure S6: Comparison of the B-B bond dissociation curve in the $B_2H_4$ molecule as calculated using the modified ReaxFF parameters (left panel) and the original parameterization results, as well as DFT benchmark data, calculated at the B3LYP/6-311G** level of theory in Ref. 10(right panel).

# $BNH_2$ and $BNH_4$ bond dissociation:

The dissociation curve of the B-N bond in the $BNH_2$ and $BNH_4$ molecules as calculated using the modified ReaxFF parameters (left panel of Fig. S7) fits well the original parameterization results, as well as DFT benchmark data, calculated at the B3LYP/6-311G** level of theory, of Ref. 8 (right panel of Fig. S7).

Figure S7: Comparison of the B-N bond dissociation curve in the $BNH_2$ and $BNH_4$ molecules as calculated using the modified ReaxFF parameters (left panel) and the original parameterization results, as well as DFT benchmark data, calculated at the B3LYP/6-311G** level of theory in Ref. 8 (right panel).

## $N_2$ bond dissociation:

The dissociation curve of the N-N bond in the $N_2$ molecule as calculated using the modified ReaxFF parameters (left panel of Fig. S8) fits well the original parameterization results, as well as DFT benchmark data of Ref. 11 (right panel of Fig. S8).
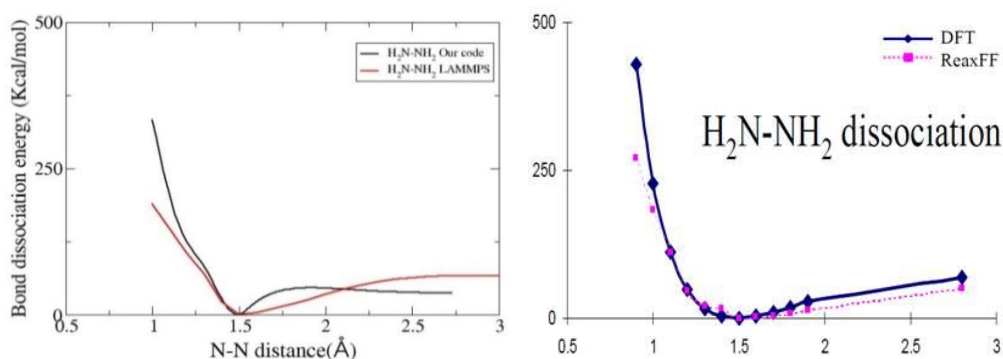


Figure S8: Comparison of the N-N bond dissociation curve in the $N_2$ molecule as calculated using the modified ReaxFF parameters (left panel) and the original parameterization results, as well as DFT benchmark data of Ref. 11 (right panel).

13

# N$_2$H$_2$ bond dissociation:

The dissociation curve of the N-N bond in the N$_2$H$_2$ molecule as calculated using the modified ReaxFF parameters (left panel of Fig. S9) fits well the original parameterization results, as well as DFT benchmark data of Ref. 11 (right panel of Fig. S9).



Figure S9: Comparison of the N-N bond dissociation curve in the N$_2$H$_2$ molecule as calculated using the modified ReaxFF parameters (left panel) and the original parameterization results, as well as DFT benchmark data of Ref. 11 (right panel).

# N$_2$H$_4$ bond dissociation:

In the case of the dissociation curve of the N-N bond of the N$_2$H$_4$ molecule the modified ReaxFF parameterization (left panel of Fig. S10) provides a somewhat worse agreement with the DFT benchmark data of Ref. 11 than the original parameterization results (right panel of Fig. S10).



Figure S10: Comparison of the N-N bond dissociation curve in the N$_2$H$_4$ molecule as calculated using the modified ReaxFF parameters (left panel) and the original parameterization results, as well as DFT benchmark data of Ref. 11 (right panel).

## H-B-H valance angle strain energy:

H-B-H valence angle strain energy as calculated using the modified ReaxFF parameters (left panel of Fig. S11) fits well the original parameterization results, as well as DFT benchmark data, calculated at the B3LYP/6-311G** level of theory, of Ref. 10 (right panel of Fig. S11).
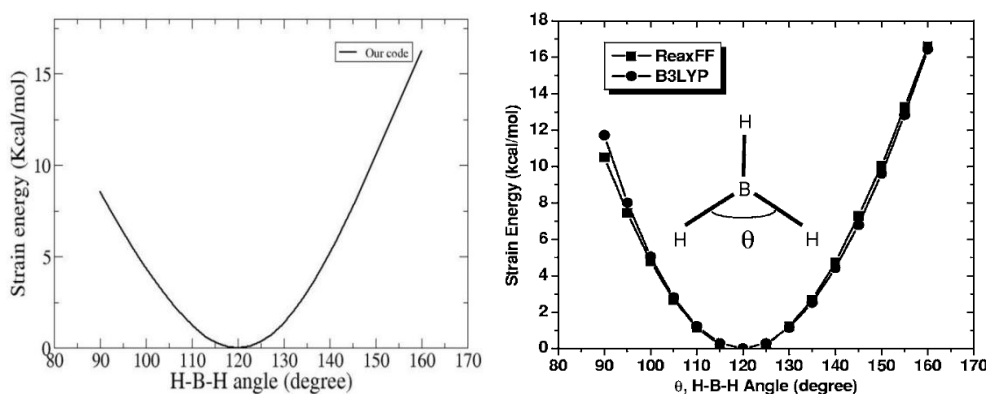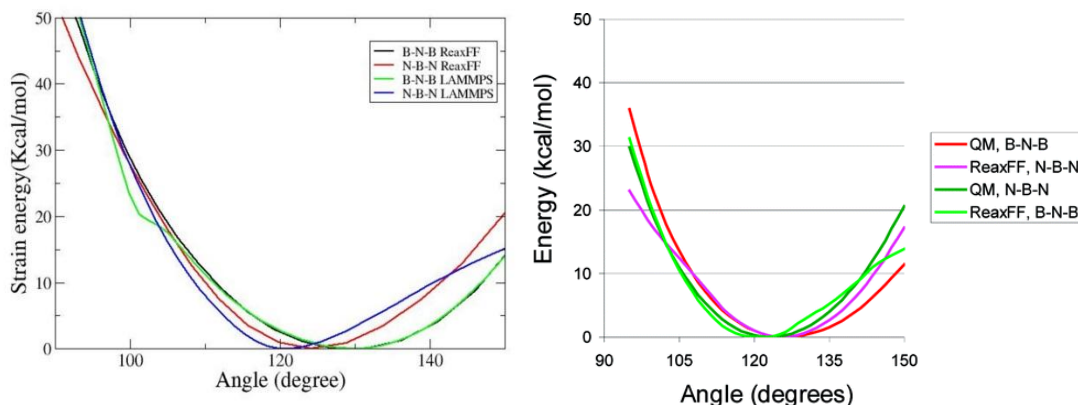


Figure S11: Comparison of the H-B-H valence angle strain energy curve as calculated using the modified ReaxFF parameters (left panel) and the original parameterization results, as well as DFT benchmark data, calculated at the B3LYP/6-311G** level of theory in Ref.10 (right panel).

## N-B-N and B-N-B valance angle strain energies:

N-B-N and B-N-B valence angle strain energies in the $H_2$-N-BH-N-$H_2$ and $H_2$-B-NH-B-$H_2$ molecules, respectively, as calculated using the modified ReaxFF parameters (left panel of Fig. S12) fits well the original parameterization results, as well as DFT benchmark data, calculated at the B3LYP/6-311G** level of theory, of Ref. 8 (right panel of Fig. S12).

Figure S12: Comparison of the N-B-N and B-N-B valence angle strain energy curves of the $H_2$-N-BH-N-$H_2$ and $H_2$-B-NH-B-$H_2$ molecules, respectively, as calculated using the modified ReaxFF parameters (left panel) and the original parameterization results, as well as DFT benchmark data, calculated at the B3LYP/6-311G** level of theory in Ref. 8 (right panel).

## $N_2H_4$ torsional strain energy:

The $N_2H_4$ torsional strain energy curve as calculated using the modified ReaxFF parameters (red curve) somewhat overestimates the DFT benchmark data (black curve), calculated at the B3LYP/6-31G** level of theory. The original ReaxFF parameterization (green curve) as implemented in the LAMMPS code, on the other hand, seems to considerably underestimate the strain energy curve.
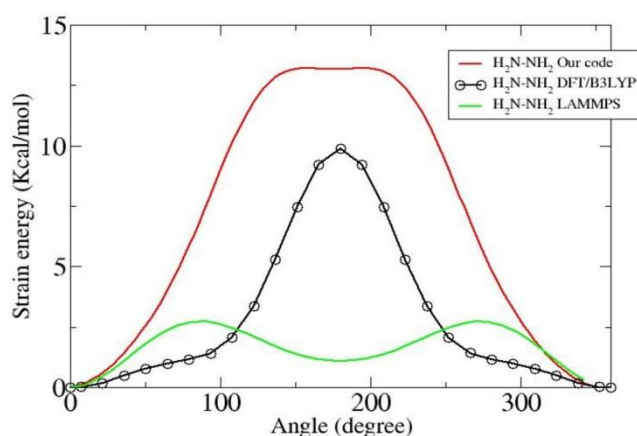


Figure S13: $N_2H_4$ torsional strain energy curve as calculated using the modified ReaxFF parameters (red-curve), the original parameterization results as implemented in the LAMMPS code (green curve), and DFT benchmark data calculated at the B3LYP/6-31G** level of theory (black curve).

## $N_2H_2$ torsional strain energy:

The $N_2H_2$ torsional strain energy curve as calculated using the modified ReaxFF parameters (red curve) fits well the DFT benchmark data (black curve), calculated at the B3LYP/6-31G** level of theory.
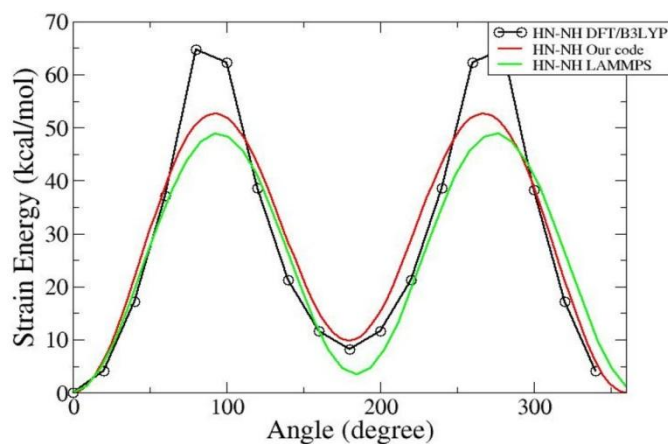


Figure S14: $N_2H_2$ torsional strain energy curve as calculated using the modified ReaxFF parameters (red-curve), DFT benchmark data calculated at the B3LYP/6-31G** level of theory (black curve) and LAMMPS (green curve).

## $BNH_4$ torsional strain energy:

The $BNH_4$ torsional strain energy curve as calculated using the modified ReaxFF parameters (red curve) corresponds well to the DFT benchmark data (black curve), calculated at the B3LYP/6-31G** level of theory. The original ReaxFF parameterization (green curve), as implemented in the LAMMPS code, considerably underestimates the strain energy.
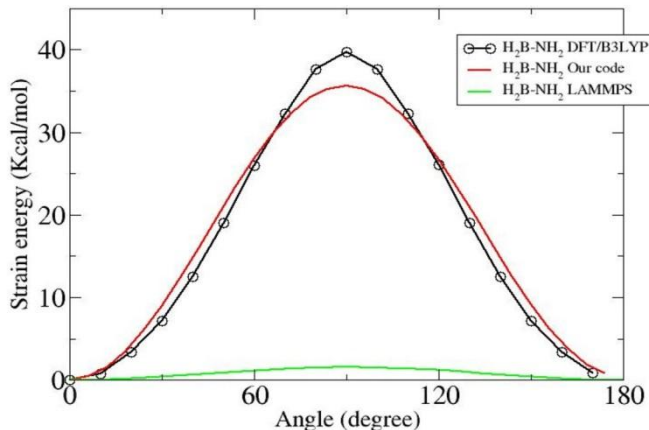
Figure S15: BNH₄ torsional strain energy curve as calculated using the modified ReaxFF parameters (red-curve), the original parameterization results as implemented in the LAMMPS code (green curve), and DFT benchmark data calculated at the B3LYP/6-31G** level of theory (black curve).

# D. Hirshfeld volumes approximation

As described in the main text, the DFT+TS-vdW calculations for the binding energy curves of the largest *h*-BN flake considered (Fig. 2(IV)) and for the sliding energy of borazine on *h*-BN (Fig. 3(a)) have been performed using an approximation of fixed values for the Hirshfeld volumes. The fixed values used in these calculations (see Tab. S18) were chosen as the average of the highest and lowest Hirshfeld volumes obtained by the full TS-vdW corrected DFT scheme, as implemented in FHI-aims, when performing the binding energy calculations of the smaller dimer systems considered.[15,16]

| $V_{rel}^N$ | $V_{rel}^B$ | $V_{rel}^H$ | $s_{R_{TS}}$ | $d_{TS}$ |
|---|---|---|---|---|
| 0.865 | 0.768 | 0.617 | 0.84 | 20.0 |

Table S18: Unit less parameters used in the TS-vdW DFT correction: Average values of the relative Hirshfeld volumes ($\frac{V_{eff}}{V_{free}}$), $d$, and $s_R$.

In order to evaluate the effect of this approximation we compare in Fig. S16 the binding energy curve of the borazine dimer as calculated using the full TS-vdW scheme and the fixed Hirshfeld volumes approach. As can be seen, the deviation along the full binding energy curve are minor with equilibrium distance and binding energy differences of 1.78 % (0.07 Å) and 5.29 % (0.39 meV/atom), respectively.
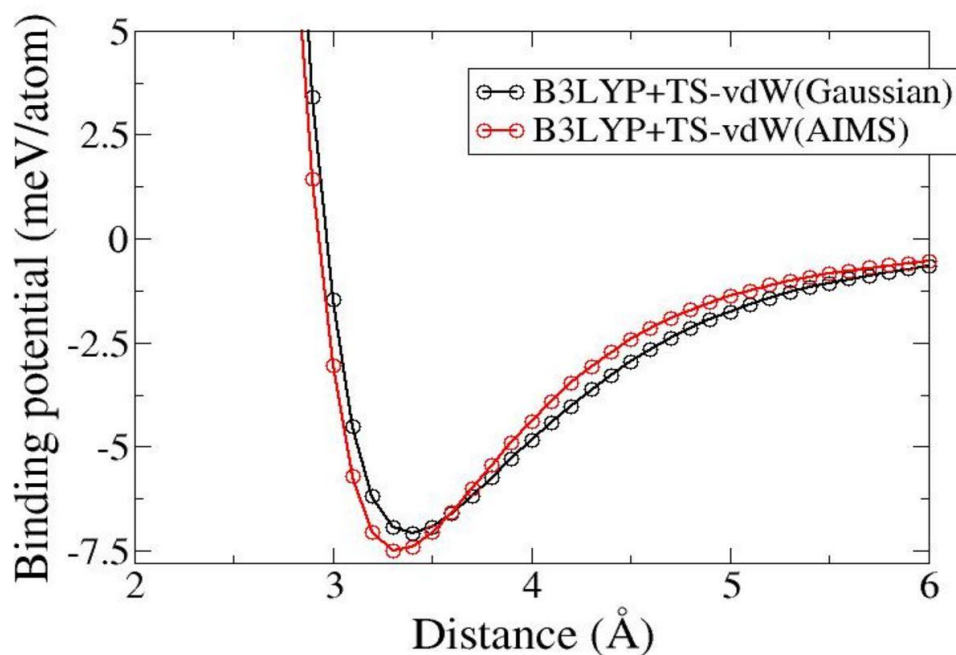


Figure S16: Binding energy curves for the borazine dimer obtained at the B3LYP level of theory using FHI-aims with the full TS-vdW scheme (black) and Gaussian + TS-vdW correction with fixed average Hirshfeld volumes (red).

Furthermore, we compare in Fig. S17 the sliding energy profile of a borazine molecule on-top of a 8x10 *h*-BN flake (see Fig. 3(d) of the main text) along the X axis direction calculated using Gaussian at the B3LYP/6-31G** level of theory and the TS-vdW correction with Min, Max, and average values of the fixed Hirshfeld volumes. As can be clearly seen, the sliding energy profiles, calculated using the various fixed Hirshfeld volumes values, differ by less than 3.94 % (0.003 eV) along the full sliding path.
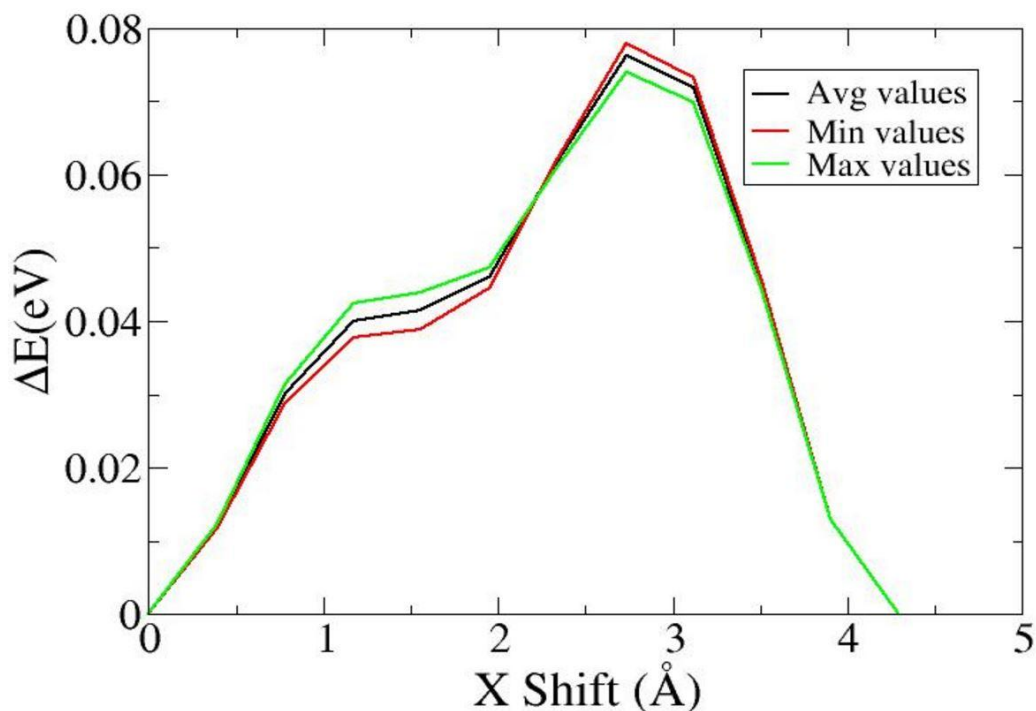
Figure S17: Sliding energy profile of a borazine molecule on-top of a 8x10 *h*-BN flake (see Fig. 3(d) of the main text) along the X axis direction, calculated using Gaussian at the B3LYP/6-31G** level of theory and the TS-vdW correction, with Min (red), Max (green) and average (black) values of the fixed Hirshfeld volumes. These values were extracted from the binding energy calculations of the small *h*-BN molecular derivative dimers calculated using the full TS-vdW scheme as implemented in FHI-aims (see main text).

# E.  Basis Set Superposition Error Tests

When performing binding energy calculations, basis set super position errors (BSSE) may become important. In order to evaluate their effect in the present study we have performed binding energy curves calculations for the borazine dimmer with and without the counterpoise (CP) BSSE correction[17,18] using both the FHI-AIMS and the Gaussian codes. These calculations have been performed using the B3LYP functional approximation with the full TS-vdW scheme and the tier-2 basis set with tight convergence conditions in the FHI-AIMS calculations and TS-vdW with fixed

Hirshfeld volumes (see discussion above) and the 6-31G** basis set in the Gaussian calculations.

The resulting binding energy curves are presented in Fig. S18. As can be seen, the binding energy curves calculated using the FHI-AIMS code and the tier-2 basis set with and without the CP correction (black and red curves) are quite similar indicating that BSSE effects her are relatively small. On the other hand, a strong BSSE effect is observed for the Gaussian calculation (green and blue curves), indicating that the 6-31G** basis set is not converged with respect to BSSE. Nevertheless, after applying the CP correction the binding energy curve calculated with Gaussian resembles those calculated with FHI-AIMS. A similar picture arises when considering the binding energies and equilibrium distances as extracted from these diagrams and presented in Tab. S19.
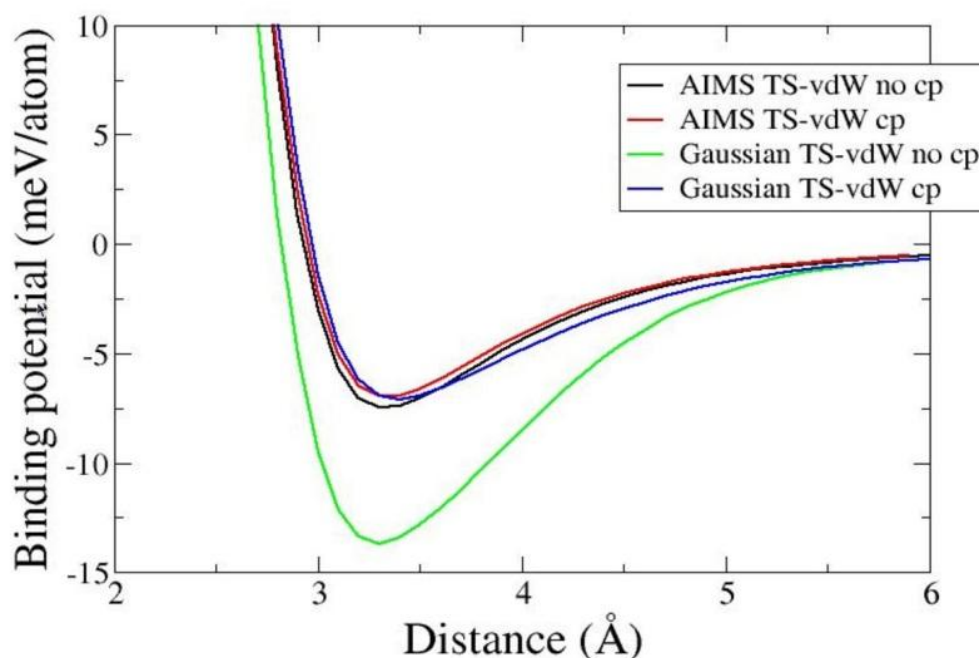


Figure S18: Binding energy curves of the borazine dimmer as calculated using the FHI-AIMS code with the full TS-vdW scheme with (red line) and without (black line) the counterpoise BSSE correction and the Gaussian suite of programs with fixed Hirshfeld volumes used for the TS-vdW scheme with (blue line) and without (green line) the counterpoise correction.

|  | AIMS TS-vdW With CP | AIMS TS-vdW No CP | Gaussian Fixed Hirshfeld With CP | Gaussian Fixed Hirshfeld No CP |
|---|---|---|---|---|
| Equilibrium Distance (Å) | 3.32 | 3.32 | 3.39 | 3.29 |
| Binding Energy (meV/atom) | -6.9 | -7.4 | -7.0 | -13.6 |

Table S19: Equilibrium distances (Å) and binding energies (meV/atom) of the Borazine dimmer as calculated using the FHI-AIMS code with the full TS-vdW scheme with and without the counterpoise BSSE correction and the Gaussian suite of programs with fixed Hirshfeld volumes used for the TS-vdW scheme with and without the counterpoise correction.

Hence, when performing the calculations presented in the main text, the Gaussian binding curves were calculated with the CP BSSE correction and the FHI-AIMS calculations have been performed without the CP BSSE correction. The sliding energy calculations have been performed with no CP BSSE correction as well as its effect there is expected to be negligible since the interlayer distance is kept fixed.

# F.   References

(1)     Mortier, W. J.; Ghosh, S. K.; Shankar, S.: Electronegativity Equalization Method for the Calculation of Atomic Charges in Molecules. *J. Am. Chem. Soc.* **1986**, *108*, 4315-4320.

(2)     Janssens, G. O. A.; Baekelandt, B. G.; Toufar, H.; Mortier, W. J.; Schoonheydt, R. A.: Comparison of Cluster and Infinite Crystal Calculations on Zeolites with the Electronegativity Equalization Method (Eem). *J. Phys. Chem.* **1995**, *99*, 3251-3258.

(3)     Njo, S. L.; Fan, J. F.; van de Graaf, B.: Extending and simplifying the electronegativity equalization method. *J. Mol. Catal. a: Chem.* **1998**, *134*, 79-88.

(4)     van Duin, A. C. T.; Dasgupta, S.; Lorant, F.; Goddard, W. A.: ReaxFF: A reactive force field for hydrocarbons. *J. Phys. Chem. A* **2001**, *105*, 9396-9409.

(5)     Bultinck, P.; Langenaeker, W.; Lahorte, P.; De Proft, F.; Geerlings, P.; Van Alsenoy, C.; Tollenaere, J. P.: The electronegativity equalization method II: Applicability of different atomic charge schemes. *J. Phys. Chem. A* **2002**, *106*, 7895-7901.

(6)     Hariharan, P. C.; Pople, J. A.: Influence of polarization functions on MO hydrogenation energies. *Theor. Chem. Acc.* **1973**, *3*, 213-222.

(7)     Frisch, M. J. T., G. W.; Schlegel, H. B.; Scuseria, G. E.; Robb, M. A.; Cheeseman, J. R.; Scalmani, G. B., V.; Mennucci, B.; Petersson, G. A.; Nakatsuji, H.;

Caricato, M.; Li, X.; Hratchian, H. P. I., A. F.; Bloino, J.; Zheng, G.; Sonnenberg, J. L.; Hada, M.; Ehara, M.; Toyota, K. F., R.; Hasegawa, J.; Ishida, M.; Nakajima, T.; Honda, Y.; Kitao, O.; Nakai, H.; Vreven, T. M., J. A.; Peralta, J. E.; Ogliaro, F.; Bearpark, M.; Heyd, J. J.; Brothers, E.; Kudin, K. N. S., V. N.; Kobayashi, R.; Normand, J.; Raghavachari, K.; Rendell, A.; Burant, J.; C.; Iyengar, S. S. T., J.; Cossi, M.; Rega, N.; Millam, J. M.; Klene, M.; Knox, J. E.; Cross, J. B.; Bakken, V. A., C.; Jaramillo, J.; Gomperts, R.; Stratmann, R. E.; Yazyev, O.; Austin, A. J.; Cammi, R. P., C.; Ochterski, J. W.; Martin, R. L.; Morokuma, K.; Zakrzewski, V. G.; Voth, G.; A.; Salvador, P. D., J. J.; Dapprich, S.; Daniels, A. D.; Farkas; Foresman, J. B.; Ortiz, J. V.; Cioslowski, J. F., D. J.: Gaussian 09, Revision A.02. Wallingford CT, 2009.

(8)      Weismiller, M. R.; van Duin, A. C. T.; Lee, J.; Yetter, R. A.: ReaxFF Reactive Force Field Development and Applications for Molecular Dynamics Simulations of Ammonia Borane Dehydrogenation and Combustion. *J. Phys. Chem. A* **2010**, *114*, 5485-5492.

(9)      Nielson, K. D.; van Duin, A. C. T.; Oxgaard, J.; Deng, W. Q.; Goddard, W. A.: Development of the ReaxFF reactive force field for describing transition metal catalyzed reactions, with application to the initial stages of the catalytic formation of carbon nanotubes. *J. Phys. Chem. A* **2005**, *109*, 493-499.

(10)      Han, S. S.; Kang, J. K.; Lee, H. M.; van Duin, A. C. T.; Goddard, W. A.: The theoretical study on interaction of hydrogen with single-walled boron nitride nanotubes. I. The reactive force field ReaxFF(HBN) development. *J. Chem. Phys.* **2005**, *123*.

(11)      Strachan, A.; van Duin, A. C. T.; Chakraborty, D.; Dasgupta, S.; Goddard, W. A., III: Shock Waves in High-Energy Materials: The Initial Chemical Events in Nitramine RDX. *Phys. Rev. Lett.* **2003**, *91*, 098301.

(12)      Hariharan, P. C. P., J. A.: Influence of polarization functions on MO hydrogenation energies. *Theor. Chem. Acc.* **1973**, *3*, 213-222.

(13)      Plimpton, S.: Fast Parallel Algorithms for Short-Range Molecular-Dynamics. *J. Comput. Phys.* **1995**, *117*, 1-19.

(14)      http://lammps.sandia.gov/index.html.

(15)      Blum, V.; Gehrke, R.; Hanke, F.; Havu, P.; Havu, V.; Ren, X. G.; Reuter, K.; Scheffler, M.: Ab initio molecular simulations with numeric atom-centered orbitals. *Comput. Phys. Commun.* **2009**, *180*, 2175-2196.

(16)      Havu, V.; Blum, V.; Havu, P.; Scheffler, M.: Efficient O(N) integration for all-electron electronic structure calculation using numeric basis functions. *J. Comput. Phys.* **2009**, *228*, 8367-8379.

(17)      Boys, S. F.; Bernardi, F.: The calculation of small molecular interactions by the differences of separate total energies. Some procedures with reduced errors (Reprinted from Molecular Physics, vol 19, pg 553-566, 1970). *Mol. Phys.* **2002**, *100*, 65-73.

(18)      Simon, S.; Duran, M.; Dannenberg, J. J.: How does basis set superposition error change the potential surfaces for hydrogen bonded dimers? *J. Chem. Phys.* **1996**, *105*, 11024-11031.